

# Automated Iterative Training of Convolutional Neural Networks for Tree Skeleton Segmentation

Keenan Granland, Rhys Newbury, David Ting and Chao Chen

*Abstract*—Training of convolutional neural networks for semantic segmentation requires accurate pixel-wise labeling. Depending on the application this can require large amounts of human effort. The human-in-the-loop method reduces labeling effort but still requires human intervention for a selection of images. This paper describes a new iterative training method: Automating-the-loop. Automating-the-loop aims to replicate the human adjustment in human-in-the-loop, with an automated process. Thereby, removing human intervention during the iterative process and drastically reducing labeling effort. Using the application of segmented apple tree detection, we compare human-in-the-loop, Self Training Loop, Filtered-Self Training Loop (semi-supervised learning) and our proposed method automating-the-loop. These methods are used to train U-Net, a deep learning based convolutional neural network. The results are presented and analyzed on both traditional performance metrics and a new metric, Horizontal Scan. It is shown that the new method of automating-the-loop greatly reduces the labeling effort while generating a network with comparable performance to both human-in-the-loop and completely manual labeling.

## I. INTRODUCTION

Recently, deep learning techniques applied to image segmentation have shown high accuracy and generalizability across a multitude of domains. By training a large amount of parameters deep learning models can learn high and low level image patterns in order to recognize and accurately segment images [1].

To train deep learning models for semantic segmentation, we require accurate pixel by pixel labeling of possibly hundreds of thousands of images for the training data sets [2]. This requires a large amount of human effort, both in terms of time and concentration. This effort is further increased for segmenting occluded objects, where human knowledge, intuition and experience plays a large role.

An example of this is detecting branches and trunks of trees, which are typically occluded by the environment. Labeling is typically done with boxes [3]. However, for some applications, such as thinning and pruning of fruit trees, the thickness of the branches is required to accurately proceed with the thinning process. As such, pixel based labeling is required [4].

To reduce labeling effort, methods such as human-in-the-loop [5] have been employed. However, this method still requires human intervention for a subset or all images. Semi-supervised processes [6] provided another method of reducing labeling effort. However, for pixel based labeling, semi-supervised processes become harder to implement due to the need for custom processes and scoring metrics [7].

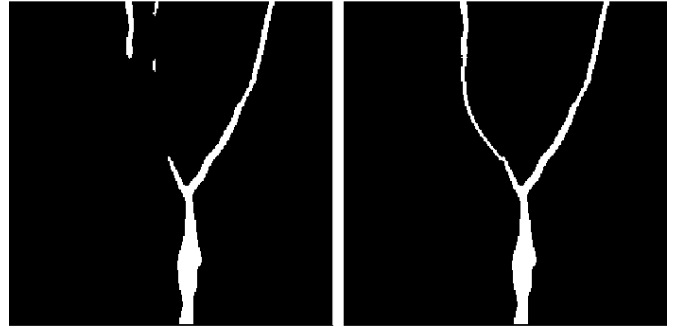


Figure 1: An example of the automated process aiming to replicate human adjustments in a human-in-the-loop iterative training process. The process starts with a possibly bad output (left) of a CNN before attempting to repair the image using a genetic algorithm (right).

In this paper, we train convolutional neural networks by attempting to replicate the human adjustments from human-in-the-loop process with an automated process (Figure 1). The application of detecting the tree skeleton of a Y-shaped apple tree is used to compare different methods of iterative training. The aim is to reduce the effort required by both minimizing the initial amount of labeling and removing human effort in an iterative training process. Many different methods are outlined, explored and compared to determine the effectiveness of each. Mean IOU, Binary Accuracy, and Boundary F1 are used to evaluate performance. In addition, a custom scoring metric is introduced to give a better comparison of the performance in this application. The contributions of this paper are:

- 1) Comparison of different iterative training methods.
- 2) Application of an automated method for repairing annotations of occluded trees.
- 3) Introduction of a new metric for axially biased images.
- 4) Application of Automating-the-Loop to successfully train a convolutional neural network.

The outline of the paper is as follows. After reviewing the literature in Section II. We introduce different methods of iterative training for convolutional neural networks in Section III. Implementation of these methods for the application of occluded apple tree detection is discussed in Section IV. Performance is then evaluated and discussed in Section V before concluding in Section VI where future work is also discussed.

## II. RELATED WORKS

Labeling data for neural networks is an important yet tedious and time consuming process, especially for pixel based

labeling, as such, researchers have explored Human-Machine Collaboration to reduce the effort (time and resources) in labeling data. For example, human-in-the-loop (HITL) assisted labeling where the human annotator modifies the output labels of a neural network, such that the labeling effort is reduced. In order to minimize the amount of labeling required, commonly, a subset of the data is selected automatically to be manually annotated, this is called active learning [8]. Ravanbakhsh *et al.* [5] use the discriminator of a generative adversarial network (GAN) to identify unreliable labels for which the export annotation is required, however, if the discriminator is confident, they use the generator to directly synthesize samples. Castrejón *et al.* [9] developed Polygon-RNN which uses a polygon annotation tool to allow the human to modify segmentation outputs to speed up the annotation by a factor 4.7 across all classes in Cityscapes [10]. Zhang and Chen [11] and Tong *et al.* [12] utilize attribute probabilities and effective relevance feedback algorithms to extract the most informative images for manual annotation from a large static pool. Zhang *et al.* [13] mine samples for active learning using a strategy based on local consistency, where local consistency is defined as the average confidence score of the pixels that are predicted as the object but the probability is less than a threshold. The outputs are then ranked and the hard samples are manually annotated. HITL labeling can also be applied to other tasks, for example, Wang *et al.* [14] develop a cost-effective active sample mining framework, where they use active labeling for low confidence samples in an object detector. While these methods reduce the labeling effort required, they still require human assistance throughout the whole process.

In projects where labeling additional images is not a viable option, other forms of semi-supervised learning have been proposed without the need for additional labeling. Semi-supervised learning is a general field in machine learning that trains supervised models using unlabeled data [6]. Its goal is to achieve better results than what can be achieved with supervised learning when there is access to a larger amount of unlabeled data. In order to achieve this many semi-supervised methodologies rely on a strong high-quality supervised baseline to build upon [6].

One of the most commonly implemented semi-supervised learning methods for CNNs is consistency regularization [15]. This method relies on the assumption that appropriate perturbations applied to unlabeled data should not significantly affect predictions compared to the unperturbed unlabeled data. Then minimizing the difference between the perturbed and unperturbed groups can directly be integrated into the CNN's loss function [16]. Another type of semi-supervised learning utilizes a discriminator to form a generative adversarial neural network. This method utilizes a discriminator trained to differentiate predictions from the model and manually annotated labels. The model's goal is then to maximize the loss of the discriminator and in doing so must learn higher level patterns and regularities in the data [17].

Another way to resolve unlabeled data is to use the model to make predictions from the unlabeled data-set, this is called pseudo-labeling. The simplest form of pseudo-labeling in

semi-supervised learning would then be to directly utilize these images in training. Whilst the simplest this has issues with self-biasing as well as perpetuating mistakes. Many semi-supervised learning models resolve the perpetuating error problem by adding a checker that chooses which of the predictions are used in training. For example, classifier models output a confidence rating which can be used to select predictions for training based on a confidence threshold [6] or custom scoring metrics external to the model can be used instead [7]. Other methods have utilized these scores not to threshold but instead to weight the training labels created from the model [18]. These methods have shown that the creation of accurate and specific scoring algorithms can be a powerful tool in enabling the use of unlabeled data for training.

### III. METHODOLOGY

#### A. Self Training Loop

The Self Training Loop (STL) retrains the CNN iteratively by adding a set of predictions to the training set each iteration. The process is shown in Figure 2.

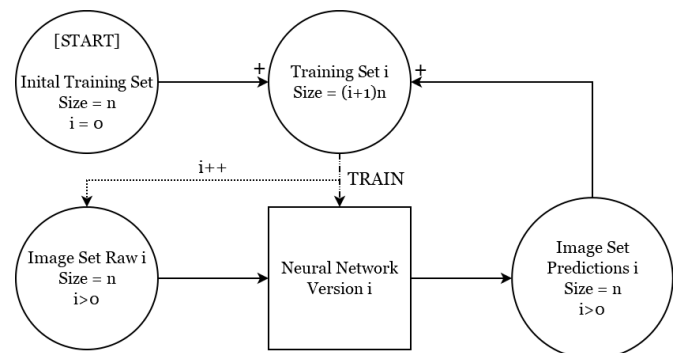


Figure 2: Self Training Loop Process

As no algorithms or humans adjust the predicted images for training, this method is explored as a comparison for all other methods and the performance of non-adjusted iterative processes.

In addition, a Filtered Self Training Loop (F-STL) is also explored. F-STL is an example of a semi-supervised learning system and will be explored as one of the baseline methods for this study. The filters implemented in F-STL should execute quickly to allow for fast training. The network is trained on an initial small training set, the full set (pool) of unlabeled images are passed through the filter. Images which pass the filter are then added to the training set and removed from the pool. This process is repeated with the larger training set and smaller pool. The process terminates when no images pass the filter ( $X_i = 0$ ). This process is shown in Figure 3.

#### B. Human-in-the-loop

The HITL method reduces the effort of labeling images, aiming to produce a convolutional neural network (CNN) with comparable performance to a CNN trained on manually labeled images. The HITL method involves a person cleaning and repairing the predicted images outputted by the CNN. The repaired images are then added to the training set and used

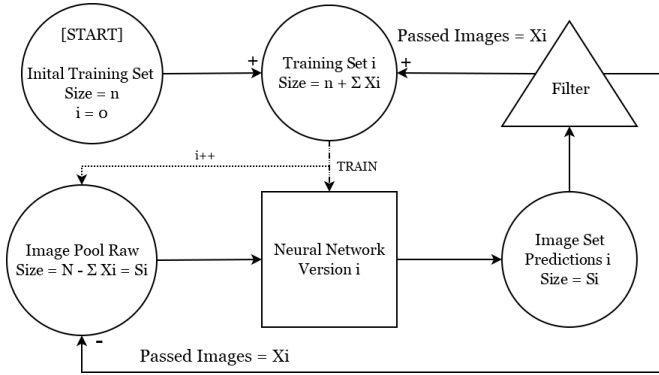


Figure 3: Filtered Self Training Loop Process

to retrain the CNN. This process occurs iteratively, where the training set size strictly increases every iteration, the process is outlined in the flow chart in Figure 4. Compared to manually labeling all images, it is estimated that HITL reduces labeling effort by a factor of 4.7 [9].

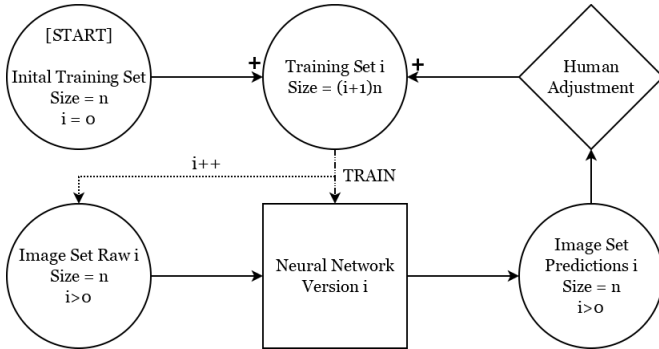


Figure 4: Human-in-the-loop Process

### C. Automating-the-Loop

Automating-the-Loop (ATL) involves replacing the Human Adjustment from Human-in-the-loop (Figure 4) with an automatic process in a similar fashion to F-STL. The automatic process is specific from the application and can involve many stages. The aim of the automated process is to replicate the human adjustment as closely as possible. This differs from traditional semi-supervised learning by actively adjusting labels using features specific from the application. This can be achieved with various methods and may involve many stages of filtering, adjustment and evaluation. This automatic process may not be able to make the adjustments, for example, if the network outputs an empty image, the automated process will not be able to make reasonable adjustments to the annotation. It should be noted that there is no requirement for this process to be completed in real-time.

## IV. IMPLEMENTATION

We present an example of the methodology for the three methods described in the Section III. We use an example of segmentation occluded trees.

For complete tree branch reconstructions, not only the visible pixels are required but the occluded areas also need

to be hallucinated. As can be seen in [4], the use of state-of-the-art segmentation networks are only able to successfully mask non-occluded regions, leaving gaps in the mask where heavy occlusions exist.

Many papers have explored adding occlusion handling, whereby the focus is to mask all visible parts correctly. Purkait *et al.* [19] focused on masking the object that exists even behind the occlusion, a term often called ‘hallucinating’ as it involves higher level thinking to predict the mask based on the object as a whole.

The labeling effort required for this application is large and requires a high amount of concentration in the labeling process due to a large area of the tree being occluded.

### A. Convolutional Neural Network Model

The neural network structure used in this project is a U-Net [20] encoder-decoder structure with a ResNet-34 [21] as the encoder. This neural network configuration has been used extensively in pixel-wise semantic segmentation problems of irregularly shaped objects [4, 22] as well as occluded segmentation [19]. The input to the network is an RGB-D image while the output is a binary mask. This neural network configuration was trained using Tensorflow and Keras and trained on a GTX1080TI using Tensorflow’s inbuilt ADAM optimizer. The images were resized from 640x480 to 256x256 and batched into batch sizes of 10 for training. The model was not pre-trained and was trained using weighted dice loss [23].

### B. Human-in-the-loop

The HITL method is applied to train the U-Net [20] with differing set sizes. In this implementation, we consider the set sizes to be fixed during training, however, this is not a requirement for this process.

In this application the main adjustments of the images were filling in small gaps, removing noise and adjusting thickness of some sections of the trees.

In order to adjust the predictions from the model, we used a tool similar to [9]. Firstly all vertices were converted into polygon points and then simplified using the Douglas-Peucker polygon simplification method [24]. These polygon points were then converted into the COCO format [25] and then adjusted in Intel’s CVAT open source annotation tool [26].

### C. Filtered Self Training Loop

In this method a blob filter is applied to the predicted images. We consider two segments: the lower 20 rows and the upper 20 rows. To meet the minimum requirements of a complete Y-shaped tree a blob must have two sections in the upper segment and one section in the lower segment. We keep the largest blob meeting these requirements, while all other blobs are filtered out. The F-STL (Figure 3) is run with an initial training set of  $n = 50$  and a pool size of  $N = 400$ . Figure 5 shows an example of the filtering process.

### D. Automating-the-Loop

An algorithm is developed that makes use of a Genetic Algorithm (GA) to repair the prediction images from the

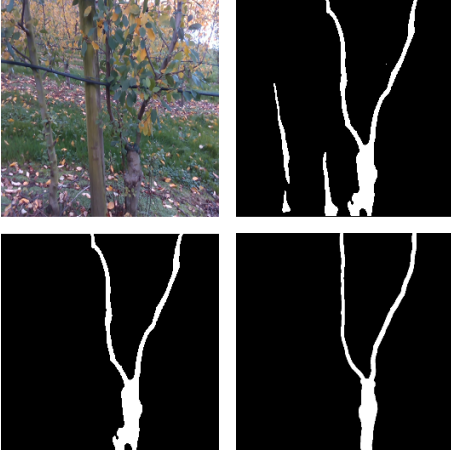


Figure 5: An example of the filtering process, the RGB image (Top Left) is passed through a CNN to generate a prediction (Top Right). The prediction is then filtered (Bottom Left). Ground truth for comparison (Bottom Right)

CNN. These processes are run using the numerical computing environment, MATLAB.

The automatic process occurs in three stages and aims to replicate a similar outcome to a human manually adjusting the predicted images. These stages in order are, filtering, tree fitting (using GA) and repairing. The complete process of retraining is outlined in Figure 6.

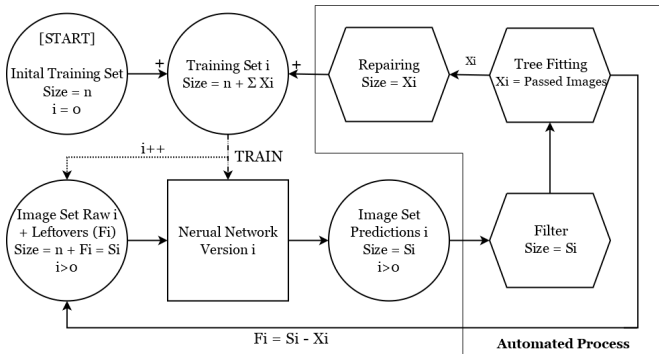


Figure 6: Automating-the-Loop Process

1) *Filtering*: The filtering process removes unwanted noise and false detections from the image before the tree fitting process. The following filters were applied:

- 1) **Small Blob Removal**: removes unwanted noise. For our image size of 256x256, small blobs less than 50 pixels are removed.
- 2) **Different Tree Detection**: removes detection of other trees. By scanning the bottom rows of the image the initial trunk position,  $t_{pos}$  was found, any blobs with an middle x position (horizontal axis) not within the range of  $\pm 100$  pixels are removed.
- 3) **False Branch Detection**: removes false branch ends from the top of the image. Blobs with a middle y position  $> 240$  and a height of  $> 5$  are removed.
- 4) **False Trunk Detection**: removes false trunks or wooden poles detected. Blobs with an x position not within the

range of  $\pm 30$  of  $t_{pos}$ , with a height of  $> 80$  and a width of  $< 15$  are removed.

2) *Fitting*: The outputs of the filtering are then given as inputs to the tree fitting, Genetic Algorithm Process.

The problem defined for the Genetic Algorithm is to fit a 14-parameter predefined Y tree skeleton to a tree skeleton. Genetic Algorithm was selected as the optimization tool as the defined problem had a large amount of variables. The skeleton is found by analyzing each row of the image. The rows are converted to average blob positions for each blob.

A Genetic Algorithm is setup according to the follow parameters, we adopt the notation used for the parameters from [27],  $N_p = 2000$ ,  $T = 800$ ,  $e_{tac} = 2$ ,  $e_{tam} = 2$ ,  $P_c = 0.8$  and  $P_m = 0.5$ .

The 14 parameters used to define the Y tree skeleton are as follows. Firstly, to define the trunk there are 4 parameters:

- $(T_{px}, 0)$  = starting point
- $(C_{p0x}, C_{p0y})$  = end point of the trunk
- $T_{pv}$  = gradient of the trunk from the point  $(T_{px}, 0)$

Using these boundary conditions the coefficients of a quadratic curve are calculated and plotted for the trunk by fitting a curve in MATLAB.

To define each branch ( $i = 1, 2$ ) there are 5 parameters:

- $(C_{p0x}, C_{p0y})$  = starting point
- $C_{pbiv}$  = gradient of the branch from  $(C_{p0x}, C_{p0y})$
- $(b_{ip1x}, b_{ip1y})$  = via point of the branch
- $(b_{ip2x}, 256)$  = end point of the branch
- $b_{ivf}$  = final gradient at the point  $(b_{ip2x}, 256)$

Using these boundary conditions the coefficients of a two connected cubic curves are calculated for each branch and plotted for each by fitting a curve in MATLAB. Figure 7 shows an example visual representation of the 14 parameters that define the Y tree skeleton.

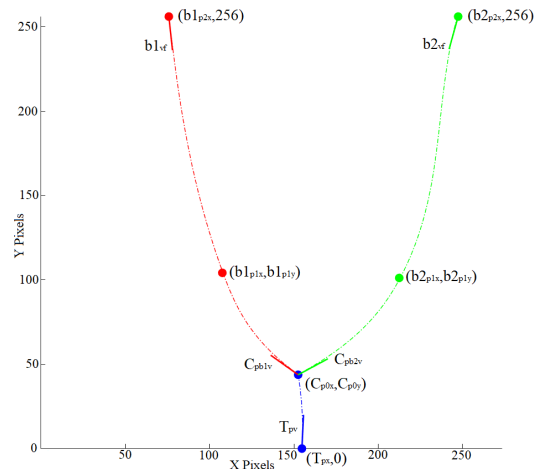


Figure 7: Visual Example of the 14 Parameters of a Y Tree Skeleton

The score is then calculated by comparing each row of the blobs in the filtered skeleton to the closest point on the corresponding row of the generated Y shaped tree skeleton. The score is calculated as the sum of the difference in position squared.

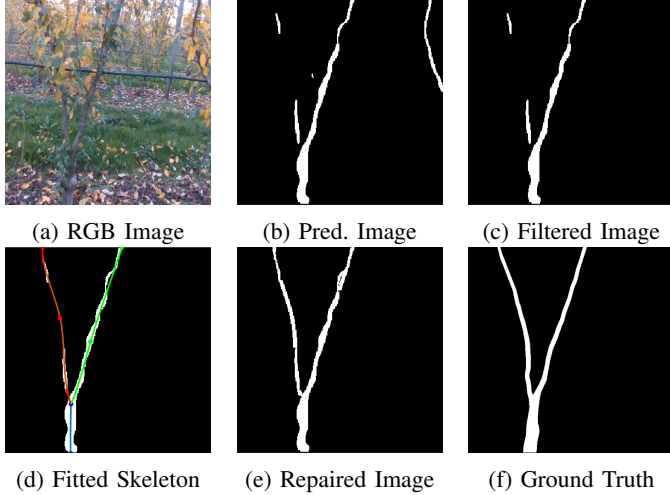


Figure 8: Automated Process Images

$$\text{Score}_t = \sum_{k=1}^{n_t} |p_t(j) - p_p(k)|^2 \quad (1)$$

$$\text{Score}_b = \sum_{k=1}^{n_b} \min(|p_{b1}(j) - p_p(k)|, |p_{b2}(j) - p_p(k)|)^2 \quad (2)$$

$$\text{Score}_{total} = \text{Score}_t + \text{Score}_b \quad (3)$$

where,  $j$ =image row,  $k$ =blob number,  $p_{st}$ =position of skeleton trunk,  $p_{sbi}$ =position of skeleton branch,  $n_t$ = total number of trunk blobs and  $n_b$ = total number of branch blobs.  $C_{p0y}$  determines the branch ( $j > C_{p0y}$ ) and trunk ( $j \leq C_{p0y}$ ) sections.

3) *Repairing*: A final filter applied to the image keeping only the largest blob, this is to remove any left over noise in the image, and the completely repaired image is created. Figure 8 shows an example of images at each stage of the process. For Figure 8c filters 1 and 2 were used to detect and remove blobs.

### E. Metrics

1) *Traditional Metrics*: To evaluate the performance of the different CNN, mean IOU (mIOU), Boundary F1 (BF1) and Binary Accuracy (Bin Acc) are used [28, 29]. We use distance threshold as 2 pixels for Boundary F1. In the application of detecting tree skeletons, where the majority of the image is the background, mIOU and Binary Accuracy score relatively closely for different predictions. For example, Figure 9b shows a ‘Good’, ‘Bad’ and Ground Truth images, the metric values are shown in Table I. While BF1 score shows a large difference, mIOU and Binary Accuracy show relatively small differences in performance. However, it is clear to see that the ‘Good’ image is more accurate than the ‘Bad’ image, compared to the Ground Truth.

2) *Horizontal Scan, Y tree Scoring*: We define an additional metric that aims to quantitatively reflects this observed qualitative difference, the Horizontal Scan (HS). HS is introduced for evaluating horizontally biased images (such as trees or building).

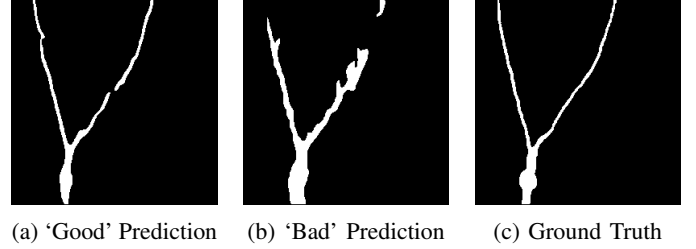


Figure 9: Image Predictions and Ground Truth

We find the error  $\mu$ , as the sum of distances between centers and the difference in thickness of each blob, with the closest ground truth blob:

$$\mu = \sum_{k=1}^n (|p_t(k) - p_p(k)| + |t_t(k) - t_p(k)|) \quad (4)$$

where,  $p_t(k)$  is the center position of the Ground Truth blob  $k$ ,  $p_p(k)$  is the center position of the closest predicted blob to  $p_t(k)$ ,  $t_t(k)$  is the thickness of the Ground Truth blob  $k$  and  $t_p(k)$  is the thickness of the corresponding predicted blob  $k$ . However, this does not account for a potential difference in the amount of blobs per row. Therefore, we need to consider the total number of errors,  $n_e$  in the amount of blobs per row:

$$n_e = \sum_{j=1}^h |n_t(j) - n_p(j)| \quad (5)$$

where  $n_t(j)$  is the number of blobs in the ground truth,  $n_p(j)$  is the number of blobs in the predicted image,  $h$  is the height of image in pixels.

We consider each error in amount of blobs as the maximum possible distance error possible in a row, the image width in pixels,  $w$ . Therefore, we defined  $\sigma$  as the error due to incorrect amount of blobs

$$\sigma = wn_e \quad (6)$$

We defined Horizontal Scan (HS) as the combination and normalization the two sources of error.

$$HS = 1 - \frac{\mu + \sigma}{w(n + n_e)} \quad (7)$$

Using the Horizontal Scan metric the score for the ‘Good’ and ‘Bad’ image (Figure 9a and 9b) are calculated and shown in Table I. The Horizontal Scan metric provides another insight into the performance of the CNN for this application.

Table I: Metric Evaluation on the ‘Good’ and ‘Bad’ predictions from Figure 9

	mIOU	Bin Acc	BF1	HS
Good	0.703	0.959	0.919	0.988
Bad	0.650	0.939	0.651	0.853

It should be noted that this method can be generalized for axially biased images, in other words it can also be used for vertically biased images by switching the axes to create ‘Vertical Scan’.

## V. RESULTS

Four different iterative methods of training are analyzed. HITL, STL, F-STL and ATL as described in Section IV, performance of the four metrics (Section IV-E) are measured at each iteration on a validation set of 50 images. It should be noted that for Trial 1 and 2, the validation metrics were calculated on the raw outputs of the CNN. Two trials are run, each with a different initial training set sizes. The ‘Manual’ method refers to manually labeled images. For the purpose of comparison, performance was analyzed iteratively.

### A. Trial 1

Trial 1 uses an initial training set size of 50 manually labeled images. The final performance of each method are outlined in Table IV, and the iterative results are shown in Figure 10.

In terms of final performance Manual and HITL perform similarly across all metrics, which is expected as they both require humans to make adjustments and approve the image. However, HITL greatly reduces the labeling effort. ATL comes next across all metrics with comparable scores to Manual and HITL, showing the effectiveness of this method. Next are F-STL and STL respectively, where STL score remains relatively constant over all metrics and F-STL makes some improvements initially before terminating.

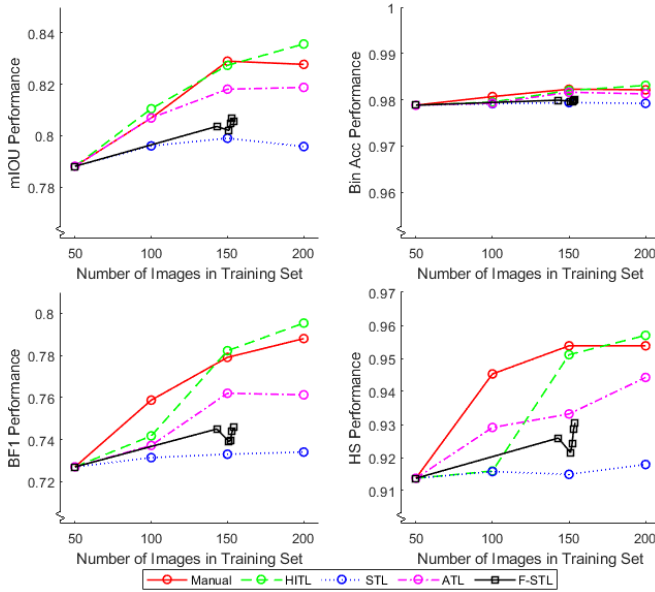


Figure 10: Iterative Performance of all metrics during Trial 1

Table II: Final Performance of all metrics in Trial 1

	mIOU	Bin Acc	BF1	HS
Manual	0.828	0.982	0.788	0.954
HITL	0.836	0.983	0.795	0.957
STL	0.796	0.979	0.734	0.918
F-STL	0.806	0.980	0.746	0.930
ATL	0.819	0.981	0.761	0.944

### B. Trial 2

Trial 2 explores how far we can push these iterative training methods by reducing the initial training set size. A set size of

20 was chosen, as this was the minimum number of images such that the network would produce reasonable initial results. The final performance of each method are outlined in Table IV, and the iterative results are shown in Figure 10.

Table III: Final Performance of all metrics in Trial 2

	IOU	Bin Acc	BF1	HS
Manual	0.815	0.981	0.776	0.934
HITL	0.810	0.980	0.750	0.926
STL	0.686	0.958	0.415	0.733
F-STL	0.764	0.974	0.667	0.865
ATL	0.787	0.979	0.723	0.923

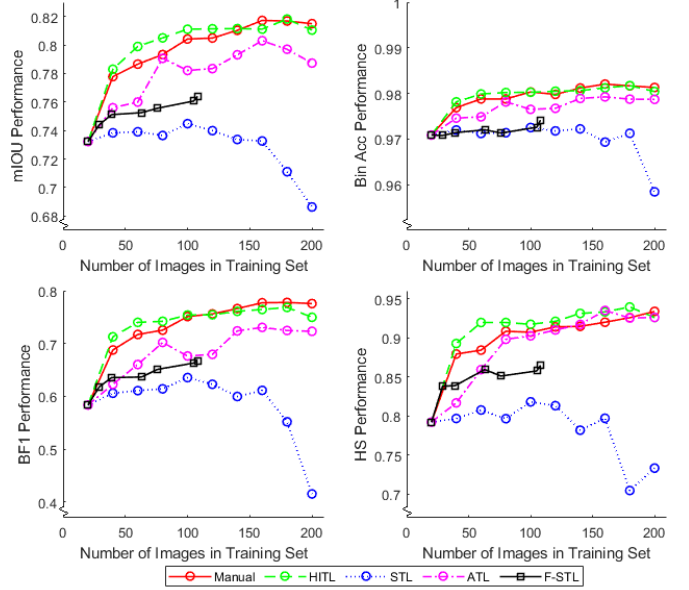


Figure 11: Iterative Performance of all metrics during Trial 2

As expected we see the same trend in performance of each method, with Manual and HITL having the best performance followed closely by ATL and then F-STL and STL respectively. However, in this trial we see a greater difference in final performance between, ATL, F-STL and STL.

ATL shows an increase of 7.56%, 23.93% and 16.88% in mIOU, BF1 and HS performance over the iterative training process. Compared to HITL, with increases of 10.6%, 28.47% and 16.86%. The ratio of performance increase to labeling effort is considered very high for ATL.

STL drops in performance over the iterations, due to the reinforcing of errors and biases. These errors and biases were not as prevalent in Trial 1 which had a higher initial training set size.

F-STL terminates earlier when compared to Trial 1, and due to the lower number of images which passed through the filter to increase the training set, has lower performance compared to Trial 1. This is reflected in Figures 10 and 11, where the process terminates with less images in the final training set, 154 for Trial 1 and 108 for Trial 2.

When comparing STL to F-STL, Trial 2 shows the significance semi-supervised training provides, in that it prevents the collapse in performance during training. Additionally, it demonstrates the importance of the initial training set size in



an iterative training process. If the initial network is not trained with enough data, it may not learn in a meaningful way such that it can generate outputs which satisfy the filter.

In terms of labeling effort STL, F-STL and ATL require only the initial training set labeled, compared to the other methods which require human intervention for all pictures. The results in this application for ATL show that it is comparable to the performance of HITL and supervised learning on all metrics and can out perform a semi-supervised learning approach on all metrics.

### C. ATL Initial Set Size

Here we compare ATL with differing initial set sizes. In addition to Trial 1 and 2, a set size of 25 analyzed. The iterative results are shown in Figure 12 where, the number following ATL refers to set size.

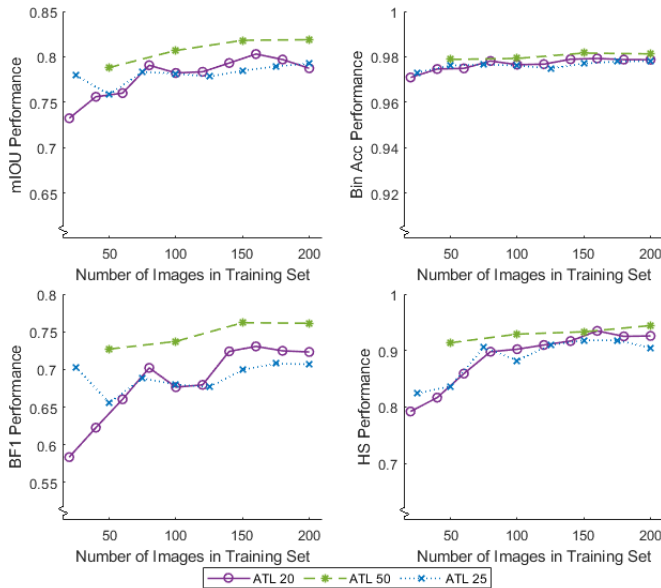


Figure 12: Iterative Performance of all ATL with different initial set sizes

For ATL 50 the performance across all metrics only slightly increases over the iterative process, inferring convergence. For ATL 20, the initial performance is relatively low. However, over the iterative process the performance approaches ATL 50 and converges, minimising the effect of the lower initial training set.

### D. Automated Process

Further analysis was completed, where the adjustment process of ATL was not just used in training, but also completed on the validation set before running the metrics.

Four different methods are analyzed, all of which require the same labeling effort. Firstly, the baseline is the validation results of the model trained only on the starting set. Automated Repairing (AR) utilizes the automated process to repair the validation results from the baseline. ATL are the validation results at the end of Trials 1 and 2. ATL and AR utilizes the automated process to repair the validation results at the end of Trials 1 and 2.

Table IV: Initial Training Set of 50

	mIOU	Bin Acc	BF1	HS
Baseline	0.788	0.979	0.727	0.914
Baseline + AR	0.7881	0.977	0.735	0.933
ATL	0.819	0.981	0.761	0.944
ATL + AR	0.816	0.981	0.759	0.958

Table V: Initial Training Set of 20

	IOU	Bin Acc	BF1	HS
Baseline	0.740	0.973	0.609	0.794
Baseline + AR	0.730	0.970	0.603	0.905
ATL	0.787	0.979	0.723	0.926
ATL + AR	0.787	0.978	0.733	0.958

Interestingly, the utilization of AR only marginally improved the results from the baseline in the case of Trial 1 and decreased the results from the Trial 2 apart from in Y-score. As this would not be during training, images where the repairing could not be completed were not removed from the validation pool, which potentially contributed to the reduced performance.

However ATL and ATL + AR both performed significantly higher than the baseline in both Trials. These results show that utilizing a repair algorithm to assist iterative training may improve performance over adding it in series to the model during execution. These results also suggest that there is minimal benefit to using the AR process during the final application. This has the additional benefit of removing real-time constraints from AR, as it would only need to be run during training.

## VI. CONCLUSION

In this paper we presented various methods for iterative training of CNNs (Section III). We introduced Automating-the-Loop, which involves attempting to replicate the human adjustment from HITL with an automated process. We introduce a new metric, Horizontal Scan, for analyzing axially biased images. In Sections IV and V, the performance of these CNNs is computed and compared. We minimized labeling effort by reducing the initial training set size to only 20 images in Trial 2. Using ATL, we successfully created a CNN with competitive performance to the manual and HITL trained CNNs. It was found that ATL process has the highest ratio of increase in performance compared to labeling effort, over the iterative process. However, this is influenced by the initial training set size, the difference in performance over the two trials shows how effective ATL is compared to a semi-supervised training method such as F-STL. Moreover using ATL to expand the training dataset outperformed AR, where the repair algorithm was used to repair outputs of the baseline model, demonstrating the effectiveness of ATL in training models specifically. Future work includes implementing the ATL process in other applications and increasing the total number of training images, exploring different automated processes and using the Horizontal Scan metric as a loss function to train CNNs.

## REFERENCES

- [1] Z.-Q. Zhao, P. Zheng, S. tao Xu, and X. Wu, "Object detection with deep learning: A review," 2019.

- [2] I. Ulku and E. Akagunduz, "A survey on deep learning-based architectures for semantic segmentation on 2d images," 2020.
- [3] H. Kang and C. Chen, "Fruit detection, segmentation and 3d visualisation of environments in apple orchards," *Computers and Electronics in Agriculture*, vol. 171, p. 105302, 2020. [Online]. Available: <http://www.sciencedirect.com/science/article/pii/S0168169919323889>
- [4] Z. Chen, D. Ting, R. Newbury, and C. Chen, "Semantic segmentation for partially occluded apple trees based on deep learning," 2020.
- [5] M. Ravanbakhsh, T. Klein, K. Batmanghelich, and M. Nabi, "Uncertainty-driven semantic segmentation through human-machine collaborative learning," 2019.
- [6] X. Zhu and A. Goldberg, *Introduction to Semi-Supervised Learning*, 2009.
- [7] Y. Ouali, C. Hudelot, and M. Tami, "Semi-supervised semantic segmentation with cross-consistency training," 2020.
- [8] B. Settles, "Active learning literature survey," *University of Wisconsin, Madison*, vol. 52, 07 2010.
- [9] L. Castrejon, K. Kundu, R. Urtasun, and S. Fidler, "Annotating object instances with a polygon-rnn," 2017.
- [10] M. Cordts, M. Omran, S. Ramos, T. Rehfeld, M. Enzweiler, R. Benenson, U. Franke, S. Roth, and B. Schiele, "The cityscapes dataset for semantic urban scene understanding," in *Proc. of the IEEE Conference on Computer Vision and Pattern Recognition (CVPR)*, 2016.
- [11] C. Zhang and T. Chen, "An active learning framework for content-based information retrieval," *IEEE Transactions on Multimedia*, vol. 4, no. 2, pp. 260–268, 2002.
- [12] S. Tong and E. Chang, "Support vector machine active learning for image retrieval," in *Proceedings of the ninth ACM international conference on multimedia*, ser. MULTIMEDIA '01, vol. 9. ACM, 2001, pp. 107–118.
- [13] X. Zhang, L. Wang, J. Xie, and P. Zhu, "Human-in-the-loop image segmentation and annotation," *Science China Information Sciences*, vol. 63, 11 2020.
- [14] K. Wang, L. Lin, X. Yan, Z. Chen, D. Zhang, and L. Zhang, "Cost-effective object detection: Active sample mining with switchable selection criteria," 2019.
- [15] J. Engelen, "A survey on semi-supervised learning," *Machine Learning*, 02 2020.
- [16] M. Sajjadi, M. Javanmardi, and T. Tasdizen, "Regularization with stochastic transformations and perturbations for deep semi-supervised learning," 2016.
- [17] P. Luc, C. Couprie, S. Chintala, and J. Verbeek, "Semantic segmentation using adversarial networks," *CoRR*, vol. abs/1611.08408, 2016. [Online]. Available: <http://arxiv.org/abs/1611.08408>
- [18] Y. Ouali, C. Hudelot, and M. Tami, "An overview of deep semi-supervised learning," 2020.
- [19] P. Purkait, C. Zach, and I. Reid, "Seeing behind things: Extending semantic segmentation to occluded regions," in *2019 IEEE/RSJ International Conference on Intelligent Robots and Systems (IROS)*, 2019, pp. 1998–2005.
- [20] O. Ronneberger, P. Fischer, and T. Brox, "U-net: Convolutional networks for biomedical image segmentation," *CoRR*, vol. abs/1505.04597, 2015. [Online]. Available: <http://arxiv.org/abs/1505.04597>
- [21] K. He, X. Zhang, S. Ren, and J. Sun, "Deep residual learning for image recognition," *CoRR*, vol. abs/1512.03385, 2015. [Online]. Available: <http://arxiv.org/abs/1512.03385>
- [22] S. L. H. Lau, E. K. P. Chong, X. Yang, and X. Wang, "Automated pavement crack segmentation using u-net-based convolutional neural network," *IEEE Access*, vol. 8, p. 114892–114899, 2020. [Online]. Available: <http://dx.doi.org/10.1109/ACCESS.2020.3003638>
- [23] C. Shen, H. R. Roth, H. Oda, M. Oda, Y. Hayashi, K. Misawa, and K. Mori, "On the influence of dice loss function in multi-class organ segmentation of abdominal ct using 3d fully convolutional networks," 2018.
- [24] B. Xiong, S. Oude Elberink, and G. Vosselman, "Footprint map partitioning using airborne laser scanning data," *ISPRS Annals of Photogrammetry, Remote Sensing and Spatial Information Sciences*, vol. III-3, pp. 241–247, 06 2016.
- [25] T.-Y. Lin, M. Maire, S. Belongie, J. Hays, P. Perona, D. Ramanan, P. Dollár, and C. Zitnick, "Microsoft coco: Common objects in context," 05 2014.
- [26] Intel. (2019) Computer vision annotation tool: A universal approach to data annotation. [Online]. Available: [software.intel.com/content/www/us/en/develop/articles/computer-vision-annotation-tool-a-universal-approach-to-data-annotation](https://software.intel.com/content/www/us/en/develop/articles/computer-vision-annotation-tool-a-universal-approach-to-data-annotation)
- [27] M. Mitchell, *An introduction to genetic algorithms*, ser. Complex adaptive systems. Cambridge, Mass.: MIT Press, 1996.
- [28] G. Csurka and D. Larlus, "What is a good evaluation measure for semantic segmentation?" *IEEE Trans. Pattern Anal. Mach. Intell.*, vol. 26, 01 2013.
- [29] Y. Sasaki, "The truth of the f-measure," *Teach Tutor Mater*, 01 2007.